

Examining T cell activation and inhibition at the nanoscale using dSTORM

SUMMARY

ONi's Nanoimager and accompanying software tools, including cloud-based CODI, offer a versatile platform to report the complex nanoscale interplay of T cell surface receptors and quantify consequences on effector function using multicolor dSTORM.

The Nanoimager enables:

- Visualization of surface protein organization with 20 nm resolution
- Characterization of protein cluster features
- Quantification of recruited effector proteins to receptors of interest
- Reporting of micro- and nanoscale protein exclusion or colocalization
- Correlation of effector recruitment with receptor cluster features and local coreceptor availability

INTRODUCTION

Regulation of protein behavior through control of spatiotemporal dynamics is a common theme throughout much of biology. Molecules may be brought together or kept segregated in order to regulate their respective effects on each other or shared effector molecules. This strategy is the foundation of how T cell activation is coordinated.

Upon activation of the T cell receptor (TCR) T cells form highly organized contacts with their corresponding antigen-presenting cell (APC), structures that are known as immunological synapses (IS)¹. Within the IS, the micro- and nanoscale distribution of proteins is tightly choreographed, with receptors and effector molecules organized into domains that range from being strictly segregated to completely overlapping. The signaling behavior of many of these proteins is heavily influenced by the nature of their nanoscale organization. For example, clustering proteins containing phosphorylatable tyrosines (e.g. ITAM/ITIM/ITSM domains) typically increases the potency of their activatory or inhibitory effects. This is due to recruitment of secondary kinases (e.g. ZAP70) or phosphatases (e.g. SHP1) that trans-phosphorylate/dephosphorylate other receptors in the same cluster². Protein cluster morphology is hence both a key determinant and helpful reporter of receptor activity. For the same reason, the relative distribution of proteins with mutually interfering behavior is also highly influential. Many co-inhibitory or co-stimulatory receptors are only able to influence their targets within a limited spatial radius e.g. references 3-4 and therefore their organization with respect to that of other receptors is of key importance. Yet, the nanoscale regulation of many T cell surface proteins is largely unstudied. Furthermore, the nanoscale characteristics of novel artificial receptors, such as chimeric antigen receptors (CARs), are typically not characterized during development. Understanding how such receptors cluster or where they distribute with respect to co-inhibitory or co-stimulatory receptors could provide key insights that inform future receptor design.

CHALLENGES

Capturing T cells in the process of IS formation and processing them in a manner that faithfully retains protein organization is not trivial. Imaging using diffraction-limited methods is not able to resolve nanoscale protein domains, whilst super-resolution methods that are not based on single-molecule detection (e.g. STED) are not well suited to molecular counting and so cannot provide quantified measurements of effector functions. Due to its approach of detecting and localizing individual molecules, direct stochastic optical reconstruction microscopy (dSTORM) is a powerful tool to report both receptor organization and quantify local protein densities. The most advanced method for IS formation that is compatible with super-resolution imaging is the use of supported lipid bilayers (SLBs), which act as planar mimics for APCs that would activate T cells *in vivo*⁵. T cells stimulated in this way can then be fixed and further processed to provide optimal conditions for imaging by dSTORM.

METHODS

Primary human T cells were isolated and stimulated with anti-CD3, anti-CD28 Dynabeads for 3 days then cultured for 4 more days without beads prior to use. Cells were cultured in the presence of 50 U/mL IL-2, which was removed 24 h prior to use. Artificial SLBs were prepared by depositing micelles of 87.5% DOPC, 12.5% DGS-NTA(Ni) onto plasma-etched glass coverslips within 6-lane imaging chambers. SLBs were blocked and washed, then incubated with recombinant His-tagged proteins of interest at the requisite concentrations to achieve the desired density. The specific combination of unconjugated proteins or proteins conjugated to different dyes was varied to suit the demands of each sample. $\sim 5 \times 10^5$ primary T cells were added to each SLB lane and incubated at 37°C for 7 min before being fixed using the ONI Discovery Kit™ for dSTORM in Cells Fixative B, para-formaldehyde (PFA) supplemented with glutaraldehyde for strong fixation. Cells were then washed, quenched, permeabilized, and blocked using the relevant reagents provided with the Discovery Kit: dSTORM in Cells. Target probing was performed with relevant primary antibodies at 4°C overnight⁶, followed by washing and incubation for 1 h at room temperature with anti-mouse and anti-rabbit secondary F(ab')₂ probes fluorescently conjugated with AZ647 and CF583R, respectively. For 2-color dSTORM, anti-TCR was imaged in the AZ647 channel, and anti-pZAP70 in the CF583R channel. For 3-color dSTORM, CD80 or PDL1 was directly conjugated to CF488A and used alongside the same anti-TCR and anti-pZAP70 probes as in 2-color dSTORM. For diffraction-limited imaging of IS formation, directly-conjugated proteins were used in the SLB (anti-CD3ε-Fab-AZ647, ICAM1-CF488A, CD80-CF568 or PDL1-CF568) and staining was performed using only directly-conjugated anti-CD45-CF405M. In all cases, after staining cells were thoroughly washed and post-fixed with PFA, then mounted in ONI's BCubed imaging buffer for dSTORM imaging. Images were collected on the Nanoimager and analyzed using ONI's CODI cloud-based platform. For 2-color dSTORM, 3000 frames of 30 ms were collected for each of the AZ647 and CF583R channels, in that order. For 3-color dSTORM, 2000 frames of 30 ms were collected for the AZ647, CF583R, and CF488A channels, in that order.

RESULTS

Throughout these experiments, an SLB system was employed to allow the functionalization of a fluid bilayer, with proteins of interest attached via His tags to nickelated lipids (FIG 1A). In all cases, SLBs were loaded with anti-CD3 ϵ -Fab at 30 molecules/ μm^2 and ICAM1 at 200 molecules/ μm^2 . This represents the minimal activatory SLB set-up, as the anti-CD3 ϵ -Fab acts in place of cognate peptide-MHC in order to bind and trigger the TCR in a clone-agnostic manner, while the ICAM1 acts as a ligand for the adhesion molecule LFA1. SLBs could also be loaded with CD80, a ligand to the costimulatory receptor CD28, and/or PDL1, ligand to the coinhibitory receptor PD1, at 200 molecules/ μm^2 .

This SLB system allowed primary human T cells to form functional IS structures, typically characterized by the central accumulation of TCR surrounded by a ring of adhesion molecules, as well as discrete domains of co-stimulatory or co-inhibitory receptors (CD80 and PDL1; FIG 1B). Other hallmarks of correct IS development were also evident, such as the enrichment of CD45 at the periphery of the contact.

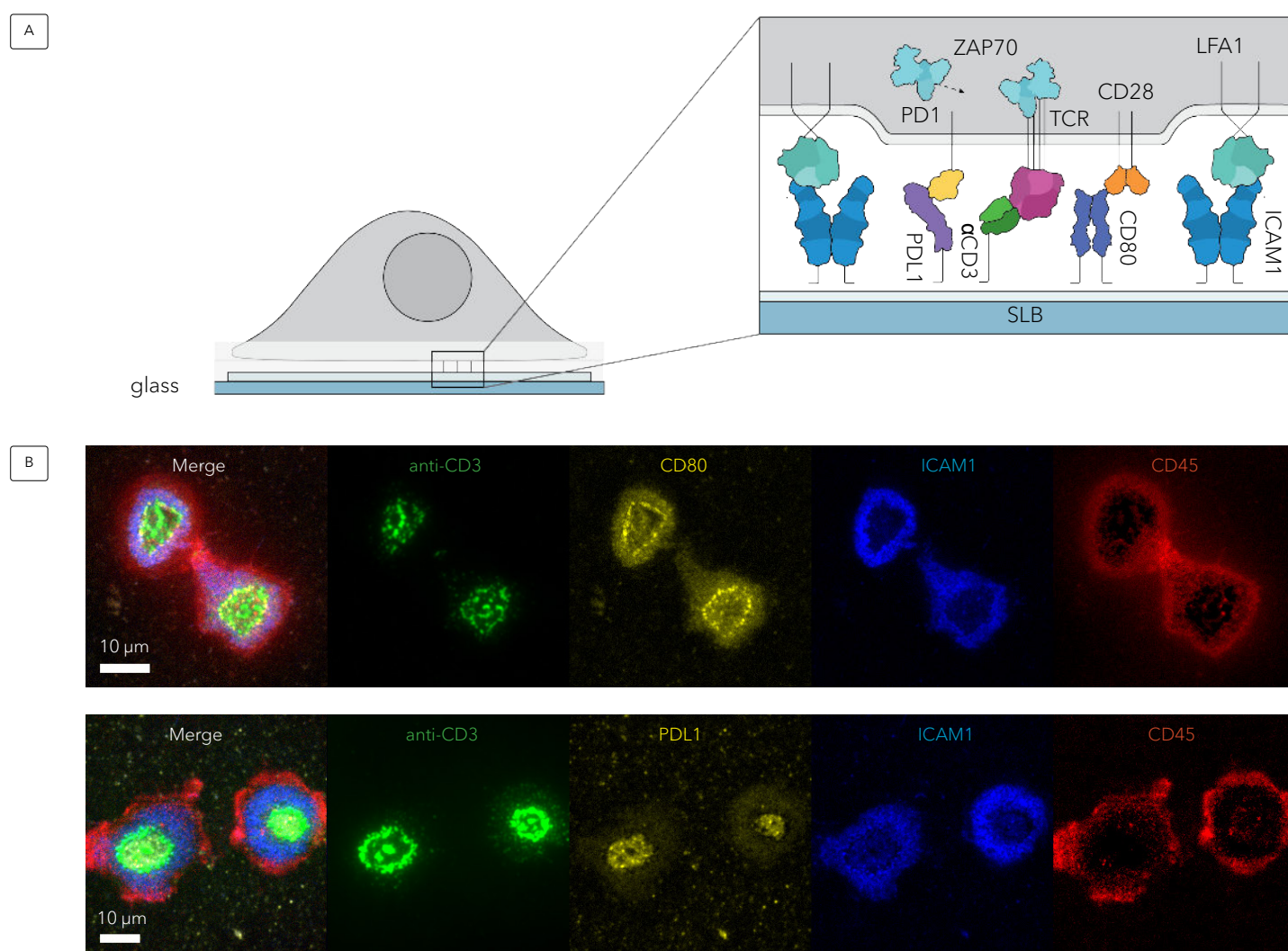


Figure 1 | A) Schematic representation of the experimental set up used, highlighting the key proteins involved. B) Representative diffraction-limited images of IS formation on SLBs containing anti-CD3 Fab, ICAM1, and either CD80 (top) or PDL1 (bottom). Characteristic compartmentalization of the IS into discrete domains is observed, including the formation of a ring of CD80 molecules surrounding the central TCR-rich zone, and the accumulation of PDL1 at the IS center.

To confirm proper activation and signaling, we analyzed the distribution of phosphorylated ZAP70 (pZAP70). Co-staining of TCR and pZAP70 exhibited the characteristic distribution of TCR signaling, wherein the majority of pZAP70 is localized towards the periphery of the IS (FIG 2A). This is because triggered TCRs form microclusters at the edge of the contact, where they recruit ZAP70 and migrate together to the center of the IS where the ZAP70 is then dissociated¹. dSTORM imaging of both proteins revealed their nanoscale organization and allowed quantification of pZAP70 recruitment to individual TCR clusters. Localizations in the TCR channel were processed using ONI's CODI cloud-based platform, wherein they were grouped into clusters according to their spatial distribution using a DBSCAN (Density-Based Spatial Clustering of Applications with Noise) algorithm with an ϵ length scale of 60 nm (FIG 2B). CODI was then able to output a wide range of parameters relating to each cluster, including their area, density, number of constituent TCR localizations, and number of pZAP70 localizations within a 100 nm radius of the TCR cluster. Large TCR clusters were more frequently distributed towards the center of the IS, whereas smaller clusters were typically more towards the periphery; consistent with the well-studied migration patterns of TCR described above.

To further reaffirm the sensitivity of our experimental system in detecting nanoscale signaling events, we also examined the behavior of the IS when treated with known regulatory proteins. In total, ~20,000 TCR clusters were identified across >15 cells for each sample condition. On a global level, the average number of pZAP70 localizations close to TCR clusters was slightly reduced by the presence of PDL1 in the SLB (FIG 2C). The presence of CD80 in the bilayer did not appreciably increase pZAP70 density around TCR clusters compared to SLBs with neither ligand, however, it was able to partially rescue the inhibitory impact of PDL1 when both ligands were added in combination (FIG 2C). In all cases, a large fraction of TCR clusters exhibited no proximal pZAP70 localizations.

Although total quantification was able to detect the inhibitory impact of PDL1, further interrogation of the data using CODI revealed the more complex processes underlying this effect. The canonical model of TCR activation suggests that non-signaling TCRs remain predominantly as single complexes or in very small clusters,

whereas productively signaling TCRs come together to form larger and slightly less dense clusters. As the TCRs migrate towards the IS center they merge into larger superclusters, where they dissociate from pZAP70 to stop the signaling activity. In line with this, when correlating proximal pZAP70 counts and TCR cluster area, it was clear that neither very small (<1,000 nm²) nor very large (>10,000 nm²) TCR clusters were typically associated closely with pZAP70, whereas those between 1,000 and 10,000 nm² had a much higher average pZAP70 count (FIG 2D). Similarly, the vast majority of pZAP70-enriched clusters had TCR densities below ~0.03 localizations/μm² (FIG 2D). These results are in line with the existing models on T cell activation. Examination of the relationship between TCR cluster area and density revealed a sharp increase in cluster density in areas smaller than ~1,000 nm², indicating that these clusters are composed of a very small number of molecules, in many cases likely just one (FIG 2E). These data are consistent with a model of TCR signal integration within the IS¹.

In order to understand the underlying process by which PDL1 causes a global reduction in pZAP70 recruitment, TCR clusters were sorted into three populations according to area: <1,000 nm², 1,000-10,000 nm², and >10,000 nm² (examples shown in FIG 2F). As expected, the middle-sized clusters had the greatest proximal pZAP70 counts in all conditions, and interestingly, the density of pZAP70 around each cluster type was broadly unaffected by the stimulation conditions (FIG 2G). This indicates that TCR clusters that reach the critical threshold for signaling are able to recruit approximately the same number of pZAP70, irrespective of the presence of CD80 or PDL1. Critically, however, when looking at the relative fractions of TCR clusters within each population it is clear that PDL1 significantly inhibits the formation of these productive clusters, as both the number of clusters and number of TCR localizations in total within the middle-sized population is substantially reduced in the presence of PDL1 (FIG 2H). CD80 induces a slight increase in the total number of TCR localizations in this population compared to conditions with neither ligand, however is able to partially restore it when both it and PDL1 are present at high densities. Overall, the differences in TCR cluster populations accounts for the entire difference in pZAP70 recruitment between conditions, and indicates that the PDL1-PD1 axis impacts TCR signaling at the very early stage, upstream of TCR cluster formation.

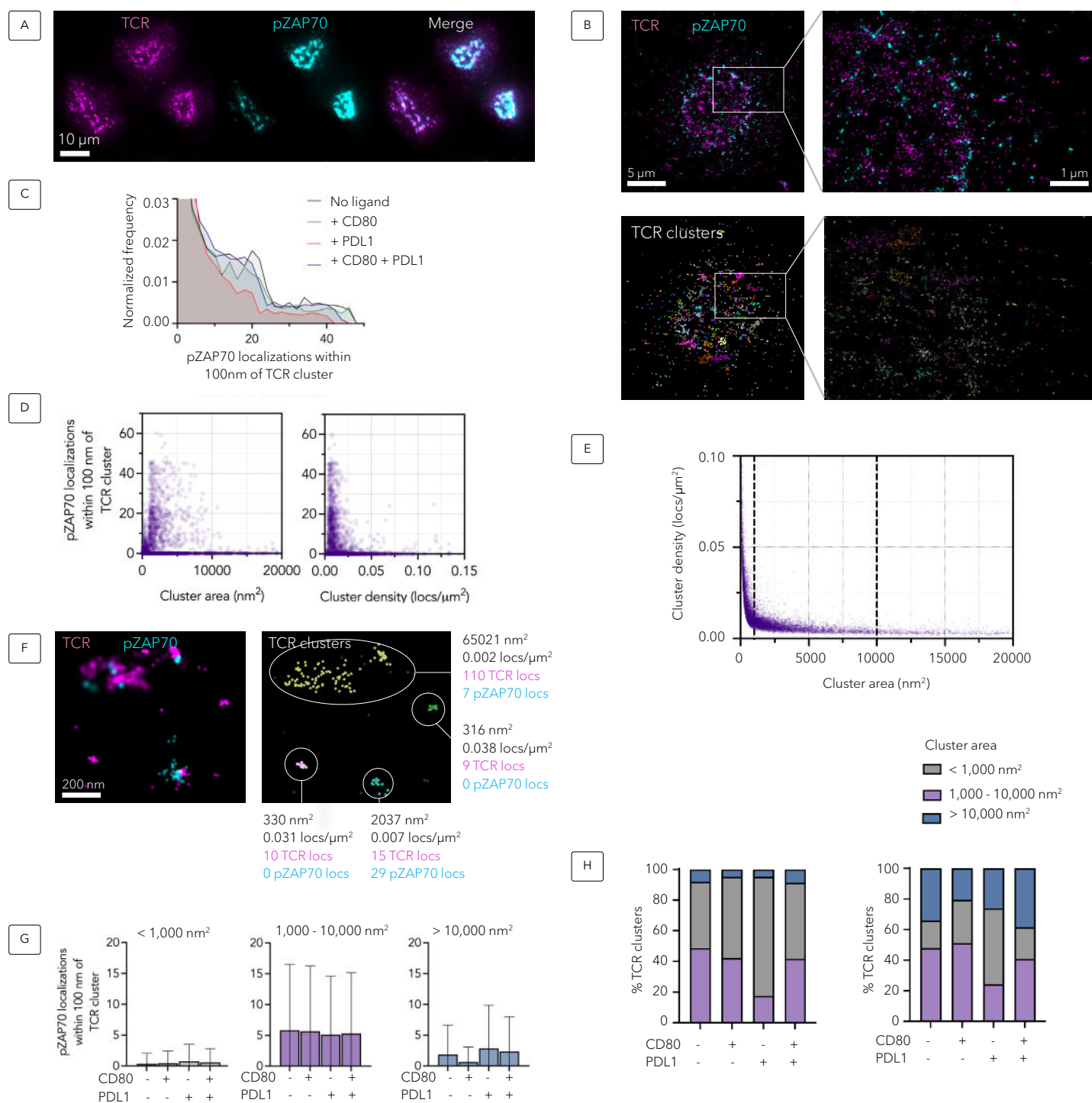


Figure 2 | Interrogation of TCR cluster formation and pZAP70 recruitment. A) Representative diffraction-limited image of TCR and pZAP70 staining within the IS. B) Example dSTORM image of TCR and pZAP70 on anti-CD3 Fab- and ICAM1-containing SLB (top) and identified TCR clusters for the same area (below). Cluster coloring is random. C) Normalized frequency histogram of the number of pZAP70 localizations within 100 nm of each identified TCR cluster ($n > 15$ cells for each condition). D) pZAP70 localizations per TCR cluster as a function of TCR cluster area (left) and density (right). Data are taken from conditions with neither CD80 nor PDL1. E) Relationship between TCR cluster area and density on SLB without CD80 or PDL1. Thick-dashed lines indicate thresholds for three cluster populations used in downstream quantification. F) Example of three different TCR cluster types; dSTORM image of both TCR and pZAP70 (left) and identified TCR clusters for the same area with their respective quantified parameters (right). G) pZAP70 localizations per TCR cluster according to cluster population area. H) Proportion of TCR clusters (top) and total TCR localizations (bottom) belonging to each area type for all tested conditions.

Expanding the imaging panel to incorporate 3-color dSTORM allows the cross-correlation of two counted proteins with the clustered TCR population. Diffraction-limited imaging of TCR, pZAP70, and CD80/PDL1 revealed that areas of substantial TCR/pZAP70 colocalization frequently correlated with CD80 signal but were segregated from

areas of PDL1 density (FIG 3A). This was borne out by 3-color dSTORM, which revealed greater overlap between regions of CD80 density with TCR/pZAP70 than for PDL1 (FIG 3B). Consequently, proximal CD80 counts exhibited a moderate positive correlation with pZAP70 counts, whereas PDL1 did not (FIG 3C), as expected from the T cell activation model.

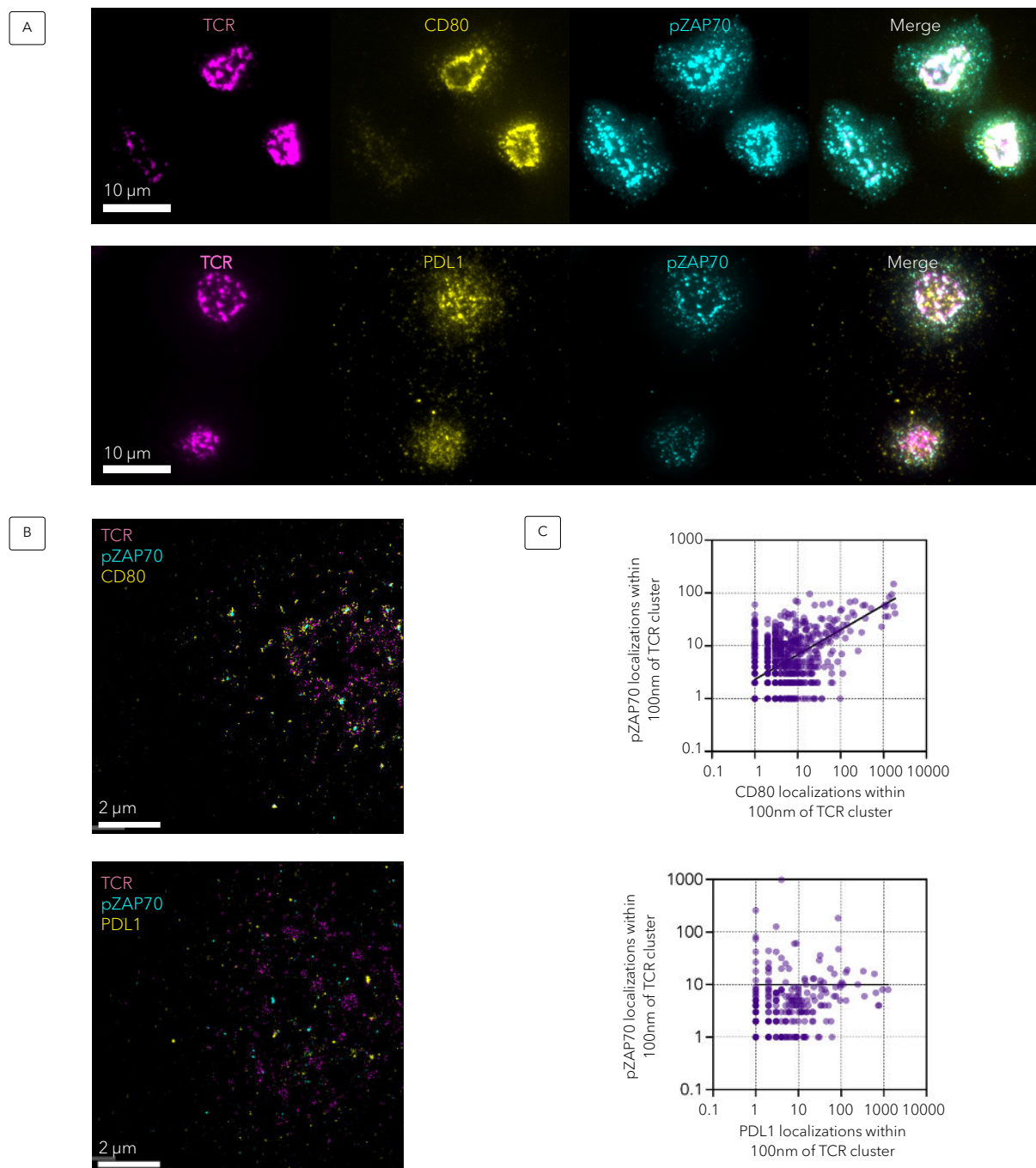


Figure 3 | Correlation between CD80/PDL1 proximity and pZAP70. A) Representative diffraction-limited images of TCR, pZAP70, and CD80 (top) or PDL1 (bottom) within the IS. B) Example single-cell dSTORM images of TCR, pZAP70, and CD80 (top) or PDL1 (bottom). C) pZAP70 localizations per TCR cluster as a function of CD80 (top) or PDL1 (bottom) localizations within 100 nm of each TCR cluster ($n > 15$ cells for each sample). Solid black lines represent a simple non-linear regression fit to the data.

In this study, advanced in-vitro reconstitution techniques were combined with dSTORM super-resolution imaging to reveal the nanoscale details of T cell activation and its disruption by inhibitory ligands. Using the Nanoimager for image acquisition and CODI for image analysis provided a straightforward, reliable workflow that could be used to investigate these complex biological processes.

SOLUTION WITH THE NANOIMAGER

The Nanoimager, which supports dSTORM imaging, in combination with the cloud-based Collaborative Discovery software CODI is able to report the nanoscale organization of proteins on T cells undergoing activation; perform quantitative measurements of effector recruitment; and reveal the relative distributions of mutually regulating proteins. This allows the complex nanoscale interplay of stimulatory and inhibitory receptors to be examined and the impact of such interplay on effector functions to be directly quantified; all outputs here are beyond the limits of conventional imaging methods. Ultimately, this could facilitate the discovery of new regulatory mechanisms, and allow the behavior and sensitivities of new, artificial receptors to be properly profiled.

REFERENCES

1. Dustin M. L. The immunological synapse. *Cancer Immunol. Res.* 2014; 2
2. Germain, R.N. T-cell signaling: The importance of receptor clustering. *Curr Biol.* 1997; 7(10)
3. Clemens L, Kutuzov M, Bayer KV, Goyette J, Allard J, Dushek O. Determination of the molecular reach of the protein tyrosine phosphatase SHP-1. *Biophys J.* 2021; 120(10)
4. Guy C, Mitrea DM, Chou P, Temirov J, Vignali KM, Liu X, Zhang H, Kriwacki R, Bruchez MP, Watkins SW, Workman CJ, Vignali DAA. LAG3 associates with TCR-CD3 complexes and suppresses signaling by driving co-receptor-Lck dissociation. *Nat Immunol.* 2022; 23
5. Calvo V, Izquierdo M Imaging polarized secretory traffic at the immune synapse in living T lymphocytes. *Front. Immunol.* 2018; 9(684)
6. Mintz MA, Felce JH, Chou MY, Mayya V, Xu Y, Shui JW, An J, Li Z, Marson A, Okada T, Ware CF, Kronenberg M, Dustin ML, Cyster JG. The HVEM-BTLA Axis Restrains T Cell Help to Germinal Center B Cells and Functions as a Cell-Extrinsic Suppressor in Lymphomagenesis. *Immunity* 2019; 51(2)